

A MESHLESS GALERKIN METHOD FOR NON-LOCAL DIFFUSION USING LOCALIZED KERNEL BASES

R. B. LEHOUCQ, F. J. NARCOWICH, S. T. ROWE, AND J. D. WARD

ABSTRACT. We introduce a meshless method for solving both continuous and discrete variational formulations of a volume constrained, non-local diffusion problem. We use the discrete solution to approximate the continuous solution. Our method is non-conforming and uses a localized Lagrange basis that is constructed out of radial basis functions. By verifying that certain inf-sup conditions hold, we demonstrate that both the continuous and discrete problems are well-posed, and also present numerical and theoretical results for the convergence behavior of the method. The stiffness matrix is assembled by a special quadrature routine unique to the localized basis. Combining the quadrature method with the localized basis produces a well-conditioned, symmetric matrix. This then is used to find the discretized solution.

1. INTRODUCTION

The contribution of our paper is a rigorous numerical analysis of a meshless method for solving a variational formulation of a volume constrained, non-local diffusion problem. Our method is non-conforming and uses a localized Lagrange basis that is constructed out of radial basis functions. The analysis presented demonstrates that the Lagrange multiplier method introduced in [6] for non-local diffusion is well-posed, in both the discrete and continuous cases. Our paper also replaces the Lagrange functions considered in [6] with local Lagrange functions as in [16], leading to dramatically reduced quadrature costs.

Non-local diffusion generalizes classical diffusion by replacing the partial differential equations with integral equations. Various models have been proposed for these cases of so-called anomalous diffusion, which include models based on integral equations and fractional derivatives. The non-local equation we consider has

Received by the editor January 11, 2016, and, in revised form, January 9, 2017, and May 12, 2017.

2010 *Mathematics Subject Classification.* Primary 45P05, 47G10, 65K10, 41A30, 41A63.

Key words and phrases. Meshless method, localized Lagrange bases, radial basis functions, non-local diffusion, volume constraint.

The first author's research was supported by the Laboratory Directed Research and Development (LDRD) program at Sandia National Laboratories. Sandia is multi-program laboratory managed and operated by Sandia Corporation, wholly a subsidiary of Lockheed Martin Corporation, for the U.S. Department of Energy's National Nuclear Security Administration under contract DE-AC04-94AL85000.

The second author's research was supported by grant DMS-1514789 from the National Science Foundation.

The third author's research was supported by grant DMS-1211566 from the National Science Foundation and Sandia National Laboratories.

The fourth author's research was supported by grant DMS-1514789 from the National Science Foundation.

applications in a variety of fields besides anomalous diffusion such as image analyses, non-local heat conduction, machine learning, and peridynamic mechanics. We apply our radial basis method to a volume constrained diffusion equation. Volume constraints replace the boundary conditions associated with classical diffusion, and are needed to demonstrate that the problem is well-posed. It also provides a link with a Markov jump process; see [8, 10] for additional information, motivation and citations to the literature.

An important distinction with the radial basis method introduced in [16] and that of this paper, is that the former method is conforming whereas the latter is non-conforming, an unavoidable aspect of a fully radial basis function method given a volume constraint. The non-conforming method of local Lagrange functions then enjoys all the benefits of a radial basis function method—error estimates and stability estimates. This represents a powerful manner in which a class of radial basis function methods can be used to approximate the solution of conventional weak formulations of classical boundary value problems.

Meshfree methods obviate the need to mesh the domain. As noted in [5], the development of meshless methods was stimulated by difficulties related to mesh generation such as when the underlying domain has a complicated geometry or when remeshing is required for time-dependent problems. Also mentioned in [5] was the potential advantages of meshless methods when a Lagrangian formulation is employed, which will be the case for this paper. Meshless methods also allow for flexibility in the selection of approximating functions, in particular non-polynomial approximating functions. In this paper the approximating spaces will be spanned by certain localized kernel bases [12, 14] that are distinguished by a rigorous approximation theory and give rise to very practical and efficient numerical methods.

A conforming discontinuous Galerkin method for a non-local diffusion problem was introduced in [9, 10] where the basis functions are given by discontinuous piecewise polynomials. More traditional finite element methods, which are applied to fractional Laplacians, are studied in [2]. Finally, in addition to finite element methods, finite difference methods are introduced and analyzed [23].

Assembly of the stiffness matrix, whether for finite element methods or for meshless methods, requires quadrature to evaluate the entries in the matrix. This is a challenging problem for three reasons: The first is that there are iterated integrals over $2n$ dimensional regions, where n is underlying the spatial dimension, to be numerically computed. The second is that the regions of integration involve partial element volumes. The third is that the quadrature method has to provide a level of accuracy commensurate with the estimations made in the rest of the problem.

Let us consider finite element quadrature methods. These require constructing meshes for those that are able to handle complicated geometries, partial volume elements, and higher dimensional regions. In general, standard finite elements will have only linear accuracy.

In contrast, the primary advantage of the meshfree quadrature methods is that entries in the stiffness matrix only require a pointwise evaluation of the kernel and multiplication by quadrature weights; complications arising from overlapping partial element volumes are irrelevant, as are complicated and/or higher dimensional regions. Consequently, our proposed method requires only information at the radial basis function nodes or centers and also yields a straightforward assembly of a stiffness matrix. As to accuracy, the numerical experiments in [16] show that

the meshless RBF method gets better than a linear rate of convergence—nearly a quadratic rate, in fact. Results in Section 6 do even better than that. This higher rate is primarily due to the underlying approximation power of the RBF theory.

The numerical analysis provided in this paper will be based on two specific classes of local Lagrange functions that will play the role of bases for the spaces U_h and Λ_h appearing in (2.7). In [14], it was shown that for either thin-plate splines or Matérn kernels on \mathbb{R}^n , local Lagrange functions with each function determined by $\mathcal{O}(\log N)^n$ points contained in a ball of radius $Kh|\log h|$ centered at a given point ξ have very rapid decay around ξ . Moreover, such functions generate very stable bases.

The theoretical development for such functions first appeared in [12] in the context of \mathbb{S}^2 . The corresponding theory for compact domains in \mathbb{R}^n appeared in [14]. Applications using these basis functions in the context of numerical solution of certain PDEs have been given in [6, 16, 17]. In particular, stability estimates for this class of functions will play a crucial role in Section 5.2 for the numerical solvability of our problem.

The remainder of the paper is organized as follows. In Section 2, the variational framework for both the continuous and discrete cases is discussed; in addition, notation to be used throughout the paper is introduced. Section 3 contains a review of the radial basis functions (RBFs) that give rise to the local Lagrange bases mentioned earlier. These bases are highly localized and computationally inexpensive. The main result is Theorem 3.5, which provides Sobolev error estimates when approximation by the quasi-interpolation operator associated with the local Lagrange basis. Section 4 establishes coercivity results for the bilinear form (2.4).

The main results of the paper are presented in Section 5. The solutions to the Euler-Lagrange formulation (2.6), for both the continuous and discrete cases, are given in Theorem 5.4 and Theorem 5.10, respectively. Finally, in Section 6 numerical results are presented. These results are in good agreement with the theoretical results discussed in Section 5.3.

2. VARIATIONAL FORMULATION

Consider a domain $\overline{\Omega} = \Omega \cup \Omega_{\mathcal{I}}$, where Ω is an inner domain, $\Omega_{\mathcal{I}}$ is the interaction region. Denote the inner product and norm on $L_2(\overline{\Omega})$ by $\langle \cdot, \cdot \rangle_{\overline{\Omega}}$ and $\|\cdot\|_{\overline{\Omega}}$, respectively. We will use similar notation for $L_2(\Omega)$ and $L_2(\Omega_{\mathcal{I}})$. The non-local operator \mathcal{L} of interest is defined by

$$(2.1) \quad \mathcal{L}u(x) := 2 \int_{\overline{\Omega}} \gamma(x, y)(u(x) - u(y)) dy, \quad u \in L_2(\overline{\Omega}).$$

The kernel $\gamma(x, y)$ is symmetric, satisfies $\gamma(x, y) \geq 0$ and is in $L_{\infty}(\overline{\Omega} \times \overline{\Omega})$. In addition, we assume that there exists an L_{∞} function $\gamma_{\delta} : [0, \infty) \rightarrow [0, \infty)$, with support in $0 \leq r \leq \delta < \infty$, such that there are constants c_1 and c_2 for which

$$(2.2) \quad c_1 \gamma_{\delta}(|x - y|) \leq \gamma(x, y) \leq c_2 \gamma_{\delta}(|x - y|), \quad x, y \in \overline{\Omega}.$$

The non-local diffusion problem that we are interested in is the analogue of a homogeneous Dirichlet problem:

$$(2.3) \quad \begin{cases} \mathcal{L}u = f, & u \in L_2(\overline{\Omega}), \quad f \in L_2(\overline{\Omega}) \\ \text{subject to } u = 0 & \text{over } \Omega_{\mathcal{I}}. \end{cases}$$

This problem can be cast into variational form. We begin by defining the bilinear form

$$(2.4) \quad a(u, v) = \int_{\bar{\Omega}} \int_{\bar{\Omega}} \gamma(x, y)(u(x) - u(y))(v(x) - v(y)) \, dx \, dy, \quad u, v \in L_2(\bar{\Omega}),$$

and the corresponding energy functional E by

$$(2.5) \quad \begin{cases} E(u) = \frac{1}{2}a(u, u) - \langle u, f \rangle_{\bar{\Omega}}, \\ \text{subject to } u = 0 \text{ over } \Omega_{\mathcal{I}}. \end{cases}$$

The constraint over the volume $\Omega_{\mathcal{I}}$ is the non-local analogue of a homogeneous Dirichlet boundary condition; the reader is referred to [10, pp. 678–680] for details and discussion. The paper [10] demonstrated that the problem of finding the minimum of the energy functional was shown to be well-posed for u in a variety of volume constrained (proper) subspaces of $L_2(\bar{\Omega})$. In [15], which also employs RBF methods, a volume constraint is imposed via a Lagrange multiplier to approximate a classical boundary condition. In contrast to these, as in [6], we minimize the functional by the method of Lagrange multipliers because the local Lagrange basis is not contained in the energy constrained space. The Lagrangian is defined as

$$L(u, \lambda) = E(u) + b(u, \lambda), \quad \text{where } b(u, \lambda) := \langle u, \lambda \rangle_{\Omega_{\mathcal{I}}}.$$

Here, $\lambda \in L^2(\Omega_{\mathcal{I}})$ is the Lagrange multiplier.

The Euler-Lagrange formulation of the problem is then: Find $u \in L^2(\bar{\Omega})$ such that

$$(2.6) \quad \begin{cases} a(u, v) + \langle v, \lambda \rangle_{\Omega_{\mathcal{I}}} = \langle v, f \rangle_{\Omega} & \text{for all } v \in L^2(\bar{\Omega}), \\ \langle u, w \rangle_{\Omega_{\mathcal{I}}} = 0 & \text{for all } w \in L^2(\Omega_{\mathcal{I}}). \end{cases}$$

We discretize this system by choosing finite dimensional subspaces $U_h \subset L^2(\bar{\Omega})$ and $\Lambda_h \subset L^2(\Omega_{\mathcal{I}})$, where

$$(2.7) \quad U_h = \text{span}\{\phi_i\}_{i=1}^N, \quad \Lambda_h = \text{span}\{\psi_k\}_{k=1}^{N_{\mathcal{I}}}.$$

We then approximate the pair (u, λ) by the discrete pair (u_h, λ_h) given by the expansions

$$u_h = \sum_{j=1}^N \alpha_j \phi_j, \quad \lambda_h = \sum_{k=1}^{N_{\mathcal{I}}} \beta_k \psi_k.$$

Inserting the expansions into (2.6) and in turn selecting v and w equal to each ϕ_i and ψ_k , respectively, determines the needed coefficients as the solution to the saddle point system

$$(2.8a) \quad \begin{pmatrix} A & B \\ B^T & 0 \end{pmatrix} \begin{pmatrix} \alpha \\ \beta \end{pmatrix} = \begin{pmatrix} b \\ 0 \end{pmatrix},$$

with matrix, vector entries given by

$$(2.8b) \quad A_{i,j} = a(\phi_i, \phi_j), \quad B_{i,k} = \langle \phi_i, \psi_k \rangle_{\Omega_{\mathcal{I}}}, \quad b_i = \langle \phi_i, f \rangle_{\Omega}.$$

3. RADIAL BASIS FUNCTIONS AND LOCALIZED KERNEL BASES

In this section, we give background material on interpolation and approximation with radial basis functions (RBFs). Radial basis functions are used to construct the approximation space for the Galerkin method we propose in Section 5.2. The interested reader should consult [24] or [11] for further details on radial basis functions and interpolation.

3.1. Radial basis functions. A radial basis function (RBF) is a radial function $\Phi(x) = \phi(|x|)$, where $\phi \in C[0, \infty)$, that is (strictly) positive definite on \mathbb{R}^n [24, Chapter 6] or (strictly) conditionally positive definite on \mathbb{R}^n , with respect to the set of polynomials $\pi_{m-1} := \pi_{m-1}(\mathbb{R}^n)$ having total degree $m-1$ or less [24, Chapter 8]. Specifically, this means that for every pairwise distinct set $X \subset \mathbb{R}^n$, with cardinality $|X| = N < \infty$, and all non-zero $a \in \mathbb{R}^N$ satisfying $\sum_{\xi \in X} a_\xi p(\xi) = 0$, for all $p \in \pi_{m-1}$, we have that

$$\sum_{\xi \in X} \sum_{\zeta \in X} \phi(|\xi - \zeta|) a_\xi a_\zeta > 0.$$

The RBFs that are conditionally positive definite with respect to π_{m-1} are said to have order $m \geq 1$. If an RBF is positive definite, it has order 0.

We will be especially interested in *thin-plate splines* (TPS) or *surface splines*, because they produce Lagrange and local Lagrange functions that are well-localized in space and have a “small” footprint among the thin-plate splines used to construct them; see [14]. For $m > n/2$, a thin-plate spline is defined by

$$(3.1) \quad \phi_m(r) := \begin{cases} r^{2m-n} & n \text{ is odd,} \\ r^{2m-n} \log r & n \text{ is even.} \end{cases}$$

For each $m > n/2$, the TPS $\phi_m(|x|)$ is an order m RBF.

An example of an RBF that has properties similar to an order m TPS, but is positive definite (order 0), is the Matérn kernel, which is defined by

$$(3.2) \quad \kappa_m(r) := CK_{m-n/2}(r) r^{m-n/2}, \quad m > n/2.$$

The label m is used to indicate the similarity to ϕ_m . Here C is a constant depending on m and n , and $K_{m-n/2}$ is a Bessel function of the second kind.

The approximation space for any RBF $\Phi(x) = \phi(|x|)$ of order m associated with a unisolvent¹ set X , which is called the set of centers, is defined by

$$(3.3) \quad V_X := \left\{ \sum_{\xi \in X} a_\xi \phi(|x - \xi|) : \sum_{\xi \in X} a_\xi p(\xi) = 0 \quad \forall p \in \pi_{m-1} \right\} + \pi_{m-1},$$

where $\pi_{-1} = \{0\}$. Specifically, each $s \in V_X$ has the form²

$$(3.4) \quad s(x) = \sum_{\xi \in X} a_\xi \phi(|x - \xi|) + \sum_{|\gamma| \leq m-1} \beta_\gamma x^\gamma,$$

where $\gamma = (\gamma_1, \dots, \gamma_n)$ is a multi-index, $|\gamma| = \gamma_1 + \dots + \gamma_n$, and $\sum_{\xi \in X} a_\xi p(\xi) = 0$ for all $p \in \pi_{m-1}$. If X is a unisolvent set for π_{m-1} and $d_\eta \in \mathbb{C}$ is given at each $\eta \in X$, there is a unique $s \in V_X$ that interpolates the d_η 's; i.e., $s(\eta) = d_\eta$. In particular, if the data are generated by a continuous function defined on a domain

¹Unisolvent with respect to π_{m-1} means every $p \in \pi_{m-1}$ is uniquely determined by its values on X .

²Bases other than $\{x^\gamma\}_{|\gamma| \leq m-1}$ may be used for π_{m-1} .

containing X , then we may take $d_\eta = f(\eta)$, and thus (uniquely) interpolate f on X . We denote the interpolant arrived at in this way by $I_X f$.

3.1.1. Geometry of the set of centers. The geometry of the centers is important for estimating the approximation quality of the RBF interpolant and for estimating the condition number of the interpolation matrix. RBF interpolation offers the advantage of not requiring regular distributions of points; arbitrarily scattered centers produce invertible interpolation matrices for positive definite functions.

Let D be a bounded, Lipschitz domain³ and let $X \subset D \subset \mathbb{R}^n$ be a set of scattered centers. We define the *fill distance* (or *mesh norm*) h , the *separation radius* q and the *mesh ratio* ρ to be:

$$(3.5) \quad h := \sup_{x \in D} \text{dist}(x, X), \quad q := \frac{1}{2} \inf_{\xi \in X} \text{dist}(\xi, X \setminus \{\xi\}), \quad \rho := \frac{h}{q}.$$

The mesh norm h is the radius of the largest ball in D that does not contain any centers. The separation radius q is the radius of the largest ball that can be placed at a center without including any other center; it is thus half of the minimal pairwise distance between the centers. Finally, we define the mesh ratio to be h/q . Obviously, $\rho \geq 1$.

The mesh ratio measures the uniformity of the distribution of X in D . The larger ρ is, the less uniform the distribution is. If ρ is “small”, then we say that the point set X is quasi-uniformly distributed, or simply that X is quasi-uniform. Geometrically, ρ controls how the centers cluster as the number of points increases. We note that for the quasi-uniformly distributed collections of centers $\{X_{h,q}\}$, which we will encounter later, we do not require any nesting of these sets of centers.

Earlier we mentioned that for a unique interpolant from V_X to exist, it was necessary that X be unisolvent with respect to π_{m-1} . For a Lipschitz domain, there is a constant $r_{m,\partial D}$ such that if $h \leq r_{m,\partial D}$, then X will be unisolvent [18, Proposition 3.5]; i.e., unisolvency holds if h is small enough.

Next, we will need a second bounded Lipschitz domain \tilde{D} and a set of centers $\tilde{X} \subset \tilde{D}$ that satisfy certain conditions. Let

$$(3.6) \quad r_h := Kh |\log h|,$$

where $K > 0$ is a parameter⁴ at our disposal. Then let $\tilde{D} \supseteq D \cup \{x \in \mathbb{R}^n : \text{dist}(x, D) \leq r_h\}$. The set of centers $\tilde{X} \subset \tilde{D}$ is chosen so that $X = \tilde{X} \cap D$, and that h , q , and ρ for \tilde{X} in \tilde{D} are approximately the same as for X in D . A method for constructing \tilde{X} is given [14, Section 2.3].

3.1.2. Approximation spaces and interpolation operators. There are two classes of functions, constructed from RBFs, that will play an important role below: Lagrange functions and local Lagrange functions.

The *Lagrange function* centered at ξ , χ_ξ , is defined to be the unique RBF interpolant satisfying $\chi_\xi(\eta) := \delta_{\xi,\eta}$, for all η in a given set of centers, which we will take to be \tilde{X} . It is obvious that the set $\{\chi_\xi : \xi \in \tilde{X}\}$ is a basis for $V_{\tilde{X}}$, and that the interpolant for a continuous function f defined on \tilde{D} is given by $I_{\tilde{X}} f = \sum_{\xi \in \tilde{X}} f(\xi) \chi_\xi$.

Local Lagrange functions are defined as follows. Let $\Upsilon_\xi := \tilde{X} \cap B_{r_h}(\xi)$. As long as h is small enough, Υ_ξ will be unisolvent with respect to π_{m-1} . The *local Lagrange*

³To avoid notation confusion, we use D rather than Ω , which is standard.

⁴On \mathbb{S}^2 for the $m = 2$ thin-plate spline, $K \approx 2.8$ worked well [12, Sections 6.3 & 7].

function at centered $\xi \in \Upsilon_\xi$ is defined to be the unique function $b_\xi \in V_{\Upsilon_\xi}$ for which $b_\xi(\eta) = \delta_{\xi,\eta}$ for all $\eta \in \Upsilon_{\xi,r}$. We remark that there are Lagrange functions centered at other points in V_{Υ_ξ} , but they play no role here. Note that each b_ξ corresponds to exactly one center in Υ_ξ , and since $\Upsilon_\xi \subset \tilde{X}$, it follows that $b_\xi \in V_{\tilde{X}}$.

We will need two additional spaces, V'_X and \tilde{V}_X ; the first is associated with Lagrange functions, and the second with local Lagrange functions:

$$(3.7) \quad V'_X := \text{span}\{\chi_\xi \in V_{\tilde{X}} : \xi \in X\},$$

$$(3.8) \quad \tilde{V}_X := \text{span}\{b_\xi \in V_{\tilde{X}} : \xi \in X\}.$$

It is important to note that, because functions in V'_X are constructed using centers from $\tilde{X} \setminus X$, not just those in X , the space V_X , which is constructed using *only* centers in X , and V'_X are *not* the same, although both are subspaces of $V_{\tilde{X}}$.

Like V_X , we are able to define an interpolation operator for V'_X . For a continuous function f defined on a domain that includes X , we let $I'_X f = \sum_{\xi \in X} f(\xi)\chi_\xi$. The formula is the superficially the same as that for $I_X f$. They are not the same, however: I_X maps to V_X while I'_X maps to $V'_X \neq V_X$.

For the local Lagrange functions, we will use *quasi-interpolants*, rather than interpolants. Given a continuous function f defined on a domain containing X , let $\tilde{I}_X f := \sum_{\xi \in X} f(\xi)b_\xi$. Because the b_ξ 's are not *full* Lagrange functions, when we evaluate $\tilde{I}_X f$ at $x = \eta \in X$, we only get $\tilde{I}_X f(\eta) = \sum_{\xi \in X} f(\xi)b_\xi(\eta)$. In general, this will not be equal to $f(\eta)$ because, unlike χ_ξ , for those $\eta \notin \Upsilon_\xi$, $b_\xi(\eta)$ will *not* be 0; thus, $\tilde{I}_X f(\eta) \neq f(\eta)$. Even so, $\tilde{I}_X f$ will behave like an interpolant; its advantage is that it can be constructed in a computationally efficient way.

3.1.3. Fractional Sobolev spaces. Throughout this paper we will use fractional, as well as integer, Sobolev spaces. Let $\beta \geq 0$, $k = \lfloor \beta \rfloor$ and let $s = \beta - k$. Note that $0 \leq s < 1$. For $1 \leq p < \infty$, various equivalent norms exist for the space $W_p^\beta(D)$ when β is fractional [3, Chapter VII]. We will use the *intrinsic* or Sobolev-Slobodeckij norm ([3, Definition 7.43], [20, Section 2])

$$\|f\|_{W_p^\beta(D)}^p := \|f\|_{W_p^k(D)}^p + \sum_{|\alpha|=k} \int_D \int_D \frac{|D^\alpha f(x) - D^\alpha f(y)|^p}{|x - y|^{n+sp}} dx dy.$$

In what follows, we will need the following lemma.

Lemma 3.1 ([20, Lemma 5.1]). *Let D, \tilde{D} be bounded Lipschitz domains, with $D \subset \tilde{D}$, $\text{dist}(\partial D, \partial \tilde{D}) > 0$, $d_1 = \text{diam}(\tilde{D})$, and let $S \subset D$ be compact, with $d_2 := \text{dist}(\partial D, S) > 0$. In addition, suppose that $f \in W_p^\beta(D)$ has support in S and that f^e extends f to all of \mathbb{R}^n by setting it equal to 0 outside of S . Then, we have*

$$(3.9) \quad \|f^e\|_{W_p^\beta(\tilde{D})} \leq \left(1 + \frac{\omega_{n-1}}{sp} (d_2^{-s} - d_1^{-s})\right) \|f\|_{W_p^\beta(D)},$$

where ω_{n-1} is the volume of the $n - 1$ sphere.

Proof. Let $\beta = k + s$, where $k = \lfloor \beta \rfloor$ and $s = \beta - k$. Repeat the proof of Lemma 5.1 in [20], keeping track of constants and adjusting for replacing \mathbb{R}^n by \tilde{D} , to see that $\|D^\alpha f^e\|_{W_p^s(\tilde{D})} \leq \frac{\omega_{n-1}}{sp} (d_2^{-s} - d_1^{-s}) \|D^\alpha f\|_{W_p^s(D)}$. In addition, we have that

$\|f^e\|_{W_p^k(\tilde{D})} = \|f\|_{W_p^k(D)}$. Hence,

$$\begin{aligned} \|f^e\|_{W_p^{k+s}(\tilde{D})}^p &= \|f\|_{W_p^k(D)}^p + \sum_{|\alpha|=k} \|D^\alpha f^e\|_{W_p^s(\tilde{D})}^p \\ &\leq \|f\|_{W_p^k(D)}^p + \left(\frac{\omega_{n-1}}{sp}(d_2^{-s} - d_1^{-s})\right)^p \sum_{|\alpha|=k} \|D^\alpha f\|_{W_p^s(D)}^p \\ &\leq \|f\|_{W_p^{k+s}(D)}^p + \left(\frac{\omega_{n-1}}{sp}(d_2^{-s} - d_1^{-s})\right)^p \|f\|_{W_p^{k+s}(D)}^p \\ &\leq \left(1 + \frac{\omega_{n-1}}{sp}(d_2^{-s} - d_1^{-s})\right)^p \|f\|_{W_p^{k+s}(D)}^p. \end{aligned}$$

Taking the p th root and using $\beta = k + s$, we arrive at (3.9). □

3.1.4. Approximation power. RBF interpolation and approximation provide excellent approximation power when X is quasi-uniformly distributed in D . For RBFs with Fourier transforms that behave like

$$(3.10) \quad c_1(1 + \|\omega\|_2^2)^{-\tau} \leq \widehat{\Phi}(\omega) \leq c_2(1 + \|\omega\|_2^2)^{-\tau}, \quad \omega \in \mathbb{R}^n,$$

or have a generalized Fourier transform that satisfies

$$(3.11) \quad c_1\|\omega\|_2^{-2\tau} \leq \widehat{\Phi}(\omega) \leq c_2\|\omega\|_2^{-2\tau}, \quad \tau \in 2\mathbb{N}, \omega \in \mathbb{R}^n \setminus \{0\},$$

where we take $\tau > n/2$, we have the approximate rates in the result below.

Theorem 3.2 ([19, Theorem 4.2]). *Suppose that ϕ is an RBF that satisfies (3.10) or (3.11) and that X is quasi-uniformly distributed in D , with separation radius q and mesh norm h . In addition, let $I_X f$ be the interpolant to f from V_X . If $\tau \geq \beta$, $\beta = k + s$ with $0 \leq s < 1$ and $k > n/2$, and if $f \in W_2^\beta(D)$, then*

$$\|f - I_X f\|_{W_2^\mu(D)} \leq Ch^{\beta-\mu} \rho^{\tau-\mu} \|f\|_{W_2^\beta(D)}, \quad 0 \leq \mu \leq \beta,$$

where $I_X f$ is given by (3.4).

The thin-plate splines satisfy (3.11), and both Matérn kernels and Wendland functions satisfy (3.10). (See [24, Sections 8.3 & 9.4].)

Corollary 3.3. *Suppose that ϕ is an RBF that satisfies (3.10) or (3.11), and that $\tau > n/2$ and $0 \leq \mu \leq \beta \leq \tau$. Also, let D, \tilde{D}, S be as in Lemma 3.1. In addition, assume that $\tilde{X} \subset \tilde{D}$, $X \subset D$, and let $X \subset \tilde{X}$ be quasi-uniform sets of centers in \tilde{D} and D , respectively, with $h_{\tilde{X}} \approx h_X \approx h$. Then, there exists $C = C_{D, \tilde{D}, S, \beta, \mu} > 0$ such that*

$$(3.12) \quad \|f - I'_X f\|_{W_2^\mu(D)} \leq Ch^{\beta-\mu} \rho^{\tau-\mu} \|f\|_{W_2^\beta(D)},$$

where $I'_X f$ is the interpolant to f defined in Section 3.1.2.

Proof. Let f^e be the extension of f to \mathbb{R}^n given in Lemma 3.1. The interpolant to f^e from $V_{\tilde{X}}$ is $I_{\tilde{X}} f^e = \sum_{\xi \in \tilde{X}} f^e(\xi) \chi_\xi(x)$. Since $f^e|_{\tilde{X} \setminus X} = 0$ and $f^e|_X = f_X$, we have $I_{\tilde{X}} f^e = \sum_{\xi \in X} f(\xi) \chi_\xi(x) = I'_X f \in V'_X \subset V_{\tilde{X}}$. Obviously, $(f^e - I_{\tilde{X}} f^e)|_D = f - I'_X f$. Consequently,

$$\|f - I'_X f\|_{W_2^\mu(D)} = \|f^e - I_{\tilde{X}} f^e\|_{W_2^\mu(D)} \leq \|f^e - I_{\tilde{X}} f^e\|_{W_2^\mu(\tilde{D})}.$$

By Theorem 3.2 and Lemma 3.1, we have

$$\|f^e - I_{\tilde{X}} f^e\|_{W_2^\mu(\tilde{D})} \leq Ch^{\beta-\mu} \rho^{\tau-\mu} \|f^e\|_{W_2^\beta(\tilde{D})} \leq Ch^{\beta-\mu} \rho^{\tau-\mu} \|f\|_{W_2^\beta(D)}.$$

Combining the two previous inequalities then yields (3.12). □

3.2. Localized kernel bases. The thin-plate splines (ϕ_m 's) and Matérn kernels (κ_m 's), which are defined in (3.1) and (3.2), respectively, give rise to Lagrange functions, the χ_ξ 's, and local Lagrange functions, the b_ξ 's, that are localized spatially and have a small footprint in the kernel basis; i.e., they use only relatively few kernels in their construction.

Throughout the rest of the paper, the ϕ_m 's and the κ_m 's will be the only RBFs used. Since their properties are very similar, we will denote either RBF by just ϕ . The ϕ_m 's are order m , so functions in the approximation space require a polynomial part from π_{m-1} . On the other hand, since the κ_m 's are order 0, functions in the the corresponding approximation space have no polynomial part. We will include the polynomial part for both RBFs, with the understanding that, for κ_m , it should be omitted.

3.2.1. Lagrange functions. Let D be a bounded Lipschitz domain, with boundary ∂D , and let X be a quasi-uniform set of centers in D . A Lagrange function centered at ξ , with ξ fixed, solves the interpolation problem $\chi_\xi(\eta) = \delta_{\xi,\eta}$ for all $\xi, \eta \in X$. Written in terms of the ϕ basis for V_X it has the expansion

$$(3.13) \quad \chi_\xi(x) = \sum_{\eta \in X} \alpha_{\eta,\xi} \phi(|x - \eta|) + \sum_{|\gamma| \leq m-1} \beta_{\gamma,\xi} x^\gamma,$$

For the thin-plate splines and Matérn RBFs, there are three important features of χ_ξ 's. The first is a decay property of the Lagrange functions. This is what makes them spatially localized. By [14, eqn. (3.5)], if $x \in D$, then there exist positive constants⁵ $\nu = \nu(\phi, n)$ and $C = C(\phi, n)$ such that

$$(3.14) \quad |\chi_\xi(x)| \leq C \rho^{m-n/2} \exp\left(-\nu \frac{|x - \xi|}{h}\right), \quad x \in D, \quad \xi \in X.$$

The second is that, by [14, eqn. (3.6)], the $\alpha_{\eta,\xi}$'s in (3.13) decay exponentially in the distance from η to ξ :

$$(3.15) \quad |\alpha_{\eta,\xi}| \leq C q^{n-2m} \exp\left(-\nu \frac{|\eta - \xi|}{h}\right), \quad \xi, \eta \in X.$$

Because of this decay, the χ_ξ 's, which are given in (3.13), require only a relatively small number of the $\phi(|\cdot - \eta|)$'s to approximately calculate them. That is, the χ_ξ 's have a small footprint in the space of kernels. In [12, Section 7], similar decay in Lagrange functions constructed using spherical basis functions was used to construct a preconditioner for solving the equations for the $\alpha_{\eta,\xi}$'s.

The third concerns stability of the Lagrange basis. We begin by defining the *synthesis* operator $T : \mathbb{C}^{|X|} \rightarrow V_X$ by $T\mathbf{a} = \sum_{\xi \in \Xi} a_\xi \chi_\xi =: s$. In other words, T takes a set of coefficients $\{a_\xi\}_{\xi \in \Xi}$ and outputs a function $s \in V_\Xi$ satisfying $s(\xi) = a_\xi$. If we use the $\ell_p(X)$ norm for $\mathbb{C}^{|X|}$ and $L_p(D)$ for V_X , then the stability of the basis, relative to these norms, is measured by comparing $\|\mathbf{a}\|_{\ell_p(X)}$ and $\|s\|_{L_p(D)}$ [14, Proposition 3.2]:

$$(3.16) \quad c \|\mathbf{a}\|_{\ell_p(X)} \leq q^{-n/p} \left\| \sum_{\xi \in X} a_\xi \chi_\xi \right\|_{L_p(D)} \leq C \rho^{m+n/p} \|\mathbf{a}\|_{\ell_p(X)}.$$

⁵To simplify the inequalities obtained from [14, eqn. (3.6)] and [14, eqn. (3.7)], we have chosen ν to be the smaller of the two decay constants used in [14]. In addition, for the $m = 2$ thin-plate spline on \mathbb{S}^2 , numerical experiments yield $\nu \approx 1.3$ [12, Section 4].

Finding the full set of Lagrange functions $\{\chi_\xi\}_{\xi \in X}$ requires solving an $N \times N$ system of equations, where $N = |X|$, to obtain the $\alpha_{\eta,\xi}$'s in (3.13). If N is large, say 30,000, then finding the χ_ξ 's essentially requires solving a $30,000 \times 30,000$ system. This is a formidable task.

The way to get around this is to make use of the exponential decay of the coefficients, given in (3.15), to truncate the coefficients used in (3.13). The result will be a set of *local* Lagrange functions, namely, the b_ξ 's introduced in Section 3.1.2. Finding the b_ξ 's requires solving a set of N relatively small linear systems, which can be done in parallel.

The properties of RBFs guarantee that the coefficients in (3.17) always can be solved for using the equations in (3.18). Letting $N_\xi = |\Upsilon_\xi| + \dim(\pi_{m-1})$, we see that the system is $N_\xi \times N_\xi$. Estimating $|\Upsilon_\xi|$ may be done by comparing volumes of B_{ξ,r_h} and of $B_{\xi,q}$, which has only a single point ξ in it. The result is

$$|\Upsilon_\xi| \approx \text{vol}(B_{\xi,r_h})/\text{vol}(B_{\xi,q}) = r_h^n/q^n = K^n \rho^n |\log h|^n.$$

The same comparison yields $N \approx \text{vol}(D)/\text{vol}(B_{\xi,q}) \approx C\rho^n h^{-n}$, equivalently, $h \approx N^{-1/n}$. It follows that $N_\xi \approx C(\log N)^n$. Since there are N centers in X , determining all of the b_ξ 's requires solving N systems that have approximately $(\log N)^n$ variables each, if the small number of β variables are ignored. These systems are symmetric and can be solved in parallel. This is a great improvement over solving the $N \times N$ system required for determining the χ_ξ 's. In fact, it is the principal reason for introducing the local Lagrange functions.

3.3. Local Lagrange functions. Local Lagrange functions, constructed from thin-plate splines or Matérn RBFs restricted to a sphere, were introduced in [12], where decay properties and quasi-interpolation convergence rates were studied. Recent work [14] has extended theoretical properties of a local Lagrange basis to bounded Lipschitz domains in \mathbb{R}^n . We now describe the properties that we will need here.

A local Lagrange function b_ξ is a Lagrange function, centered at $\xi \in X$, for $\Upsilon_\xi := \tilde{X} \cap B_{\xi,r_h}$. It has the form

$$(3.17) \quad b_\xi(x) := \sum_{\eta \in \Upsilon_\xi} \alpha_{\eta,\xi} \phi(|x - \eta|) + \sum_{|\gamma| \leq m-1} \beta_{\gamma,\xi} x^\gamma,$$

where the coefficients are uniquely determined by the equations

$$(3.18) \quad b_\xi(\eta) = \delta_{\xi,\eta}, \quad \xi \in X, \quad \eta \in \Upsilon_\xi \quad \text{and} \quad \sum_{\eta \in \Upsilon_\xi} \alpha_{\eta,\xi} p(\eta) = 0, \quad \forall p \in \pi_{m-1}.$$

The local Lagrange functions have decay properties similar to the Lagrange functions, although the rates are polynomial rather than exponential in the mesh norm h . Let J be given by

$$(3.19) \quad J := \begin{cases} K\nu/2 + 2n - 4m - 1, & \text{Matérn RBF,} \\ K\nu/2 + n - 5m, & \text{Thin-plate spline.} \end{cases}$$

Then, by [14, Lemmas 4.7 & 4.9], with $\sigma = 0$ and $p = \infty$, we have, for $x \in D$ and $\xi \in X$, $|b_\xi(x) - \chi_\xi(x)| \leq C_\rho h^J$. With a little work, this can be used to obtain the bound below, which again holds for $x \in D, \xi \in X$:

$$(3.20) \quad |b_\xi(x)| \leq C_\rho \left(1 + \frac{|x - \xi|}{h}\right)^{-J}.$$

In addition to the decay result above, there is also a result concerning stability [14, Proposition 411],

$$(3.21) \quad c \|\mathbf{a}\|_{\ell_p(X)} \leq q^{-n/p} \left\| \sum_{\xi \in X} a_\xi b_\xi \right\|_{L_p(D)} \leq C \rho^{m+n/p} \|\mathbf{a}\|_{\ell_p(X)},$$

which holds if $K > (10m - 2)/\nu$ and $1 \leq p \leq \infty$.

Recall that the space associated with local Lagrange functions having ξ in X is defined by $\tilde{V}_X = \text{span}\{b_\xi : \xi \in X\}$. The stability estimate in (3.21) implies that $\{b_\xi : \xi \in X\}$ is linearly independent. Consequently, it is a basis for \tilde{V}_X .

There is another result that we will need below. It involves an inequality established in the course of proving [14, Proposition 4.11].

Lemma 3.4. *Suppose that $K > (10m - 2)/\nu$. For $0 \leq \sigma \leq m - (n/2 - n/p)_+$ and $1 \leq p < \infty$ (or $\sigma \in \mathbb{N}$ and $0 \leq \sigma < m - n/2$ when $p = \infty$), then there is a constant $C = C(\sigma, p, m, D) > 0$ such that we have*

$$(3.22) \quad \left\| \sum_{\xi \in X} a_\xi (b_\xi - \chi_\xi) \right\|_{W_p^\sigma(D)} \leq Ch^{J-n(\frac{p-1}{p})} \|\mathbf{a}\|_{\ell_p(X)}.$$

Proof. The inequality was established in the proof of [14, Theorem 4.10]; it is [14, eqn. (4.14)]. □

3.3.1. Quasi-interpolants and approximation power. Our aim now is to extend Corollary 3.3 to the quasi-interpolant case, again with centers outside of D . This plays a role in error estimates for the non-local diffusion problems discussed later and also in the quadrature method given at the end of this section.

Theorem 3.5. *Let $k \in \mathbb{N}$, $0 \leq s < 1$, and $n/2 < \beta = k + s \leq m$. Suppose that ϕ is a thin-plate spline ϕ_m or a Matérn kernel κ_m . If $f \in W_2^\beta(D)$ is compactly supported in D and $0 \leq \mu \leq \beta$, then there is an h_0 and a sufficiently large K such that for all $h \leq h_0$ we have*

$$(3.23) \quad \|f - \tilde{I}_X f\|_{W_2^\mu(D)} \leq Ch^{\beta-\mu} \|f\|_{W_2^\beta(D)}.$$

Proof. Let $x \in D$ and form both the interpolant $I'_X f = \sum_{\xi \in X} f(\xi) \chi_\xi(x) \in V'_X$ and the quasi-interpolant $\tilde{I}_X f(x) = \sum_{\xi \in X} f(\xi) b_\xi(x) \in \tilde{V}_X$ for f . We have,

$$\|f - \tilde{I}_X f\|_{W_2^\mu(D)} \leq \underbrace{\|f - I'_X f\|_{W_2^\mu(D)}}_A + \underbrace{\|I'_X f - \tilde{I}_X f\|_{W_2^\mu(D)}}_B.$$

By Corollary 3.3, we have $A \leq Ch^{\beta-\mu} \rho^{\tau-\mu} \|f\|_{W_2^\beta(D)}$. To estimate B , note that $I'_X f - \tilde{I}_X f = \sum_{\xi \in X} f(\xi) (\chi_\xi(x) - b_\xi(x))$. Applying Lemma 3.4, with $a_\xi = f(\xi)$, yields

$$(3.24) \quad B = \left\| \sum_{\xi \in X} f(\xi) (b_\xi - \chi_\xi) \right\|_{W_2^\mu(D)} \leq Ch^{J-\frac{n}{2}} \|f\|_{\ell_2(X)},$$

where J is given in (3.19). By (3.16), with $a_\xi = f(\xi)$, we have

$$\|f\|_{\ell_2(X)} \leq c^{-1} q^{-\frac{n}{2}} \|I'_X f\|_{L_2(D)} \leq c^{-1} \rho^{\frac{n}{2}} h^{-\frac{n}{2}} (\|I'_X f - f\|_{L_2(D)} + \|f\|_{L_2(D)}).$$

Applying the estimate on A for the $\mu = 0$ case and using the fact that $\|f\|_{L_2(D)} \leq \|f\|_{W_2^\beta(D)}$, we see that $\|f\|_{\ell_2(X)} \leq Cq^{-\frac{n}{2}} \|f\|_{W_2^\beta(D)} = C\rho^{\frac{n}{2}} h^{-\frac{n}{2}} \|f\|_{W_2^\beta(D)}$. Using

this to bound the right side of (3.24) results in $B \leq C\rho^{n/2}h^{J-n}\|f\|_{W_2^\beta(D)}$. Choose K in (3.19) so large that $J \geq \beta - \mu + n$. This yields

$$(3.25) \quad B \leq C\rho^{n/2}h^{\beta-\mu}\|f\|_{W_2^\beta(D)}.$$

Adding A and B then yields (3.23). □

For future reference, we wish to note that these error estimates lead to estimates for the distance of f to $\text{span}\{b_\xi : \xi \in X\}$. Since $\text{dist}_{L_2(D)}(f, \text{span}\{b_\xi : \xi \in X\}) \leq \|f - \tilde{I}_X f\|_{L_2(D)}$, we have, for $f \in W_2^\beta(D)$ having compact support in D ,

$$(3.26) \quad \text{dist}_{L_2(D)}(f, \text{span}\{b_\xi : \xi \in X\}) \leq Ch^\beta\|f\|_{W_2^\beta(D)}.$$

Remark 3.6. There are two ways in which Theorem 3.5 is likely to be able to be improved: better rates and removal of the requirement for compact support. As we mentioned earlier, for RBF interpolation of sufficiently smooth functions, Schaback [21, Theorem 5.1] obtained a rate double that given earlier in Theorem 3.2. Hangelbroek [13, Corollary 5.2] established a result showing this phenomenon to be true using the basis $\{\chi_\xi\}$, for functions in certain Besov spaces. Something similar is certainly true for Sobolev spaces, and will be dealt with in future work. As to the support requirement, we believe that it is an artifact of the method of proof and is unnecessary, in view of the result [19, Theorem 4.2] holding when all of the centers are inside of D . Showing this conjecture holds is an open problem. In Section 6, we will discuss numerical evidence supporting our conjectures.

3.3.2. Quadrature using quasi-interpolants. We now turn to a quadrature formula for $f \in W_2^\beta(D)$. We will require this formula to be exact for all functions in \tilde{V}_X . To derive it, let $s = \sum_{\xi \in X} a_\xi b_\xi$ and observe that this requirement implies that $\int_D s(x)dx = \sum_{\xi \in X} a_\xi \int_D b_\xi(x)dx$. If we replace s by the quasi-interpolant $\tilde{I}_X f$, then we have

$$(3.27) \quad Q_X(f) := \int_D \tilde{I}_X f(x)dx = \sum_{\xi \in X} f(\xi)w_\xi, \text{ where } w_\xi := \int_D b_\xi(x)dx.$$

A straightforward application of Theorem 3.5 yields the following error estimates for the quadrature formulas.

Proposition 3.7 ([16, Lemma 2]). *Under the conditions of Theorem 3.5, with $\beta \in \mathbb{R}$, $n/2 < \beta \leq m$, $\mu = 0$, and $f \in W_2^\beta(D)$ having compact support in D , we have*

$$(3.28) \quad \left| \int_D f(x)dx - Q_X(f) \right| \leq Ch^\beta\|f\|_{W_2^\beta(D)}.$$

We close this section by deriving a formula for the weights in the quadrature formula. In the formula $w_\xi := \int_D b_\xi(x)dx$, we replace b_ξ by the right side of (3.17) and integrate; this yields:

$$(3.29) \quad w_\xi = \sum_{\eta \in X} \alpha_{\eta,\xi} \underbrace{\int_D \phi(x - \eta)dx}_{J(\eta)} + \sum_{|\gamma| \leq m-1} \beta_{\gamma,\xi} \underbrace{\int_D x^\gamma dx}_{J_\gamma}.$$

It follows that if we can calculate the $J(\eta)$'s and J_γ we can obtain the weights from the coefficients in (3.17). When D is a polygonal domain and ϕ a thin-plate spline, there is a simple, exact, analytical formula for $J(\eta)$, which we derive in Appendix A. Employing this formula greatly reduces the cost of finding the weights.

4. COERCIVITY

Now we will need various coercivity results for the quadratic form (2.4). (At this point, we again use Ω , $\bar{\Omega}$, and $\Omega_{\mathcal{I}}$ as in Section 2.) We begin with the following lemmas.

Lemma 4.1. *Let $u \in L_2(\bar{\Omega})$. Suppose that $0 \leq \varepsilon < 1$. If $|\int_{\Omega_{\mathcal{I}}} u(x)dx| \leq \varepsilon|\Omega_{\mathcal{I}}|^{1/2}\|u\|_{\Omega_{\mathcal{I}}}$, then*

$$(4.1) \quad \frac{1}{\sqrt{|\bar{\Omega}|}} \left| \int_{\bar{\Omega}} u(x)dx \right| \leq (\sqrt{1-\varrho} + \sqrt{\varrho}\varepsilon) \|u\|_{\bar{\Omega}}, \quad \varrho := \frac{|\Omega_{\mathcal{I}}|}{|\bar{\Omega}|}.$$

Furthermore, if $0 < t \leq 1$ and $\varepsilon \leq \frac{(1-t)\sqrt{\varrho}}{1+\sqrt{1-\varrho}}$, then

$$(4.2) \quad \frac{1}{\sqrt{|\bar{\Omega}|}} \left| \int_{\bar{\Omega}} u(x)dx \right| \leq \left(1 - \frac{t\varrho}{1 + \sqrt{1-\varrho}} \right) \|u\|_{\bar{\Omega}}.$$

Proof. Since $\int_{\bar{\Omega}} u(x)dx = \int_{\Omega} u(x)dx + \int_{\Omega_{\mathcal{I}}} u(x)dx$, by Schwarz’s inequality, we have that

$$\left| \int_{\bar{\Omega}} u(x)dx \right| \leq |\Omega|^{1/2}\|u\|_{\Omega} + \varepsilon|\Omega_{\mathcal{I}}|^{1/2}\|u\|_{\Omega_{\mathcal{I}}} \leq (|\Omega|^{1/2} + \varepsilon|\Omega_{\mathcal{I}}|^{1/2}) \|u\|_{\bar{\Omega}}.$$

Divide both sides above by $|\bar{\Omega}|^{1/2}$. Note that $|\Omega| = |\bar{\Omega}| - |\Omega_{\mathcal{I}}|$, so $|\Omega|/|\bar{\Omega}| = 1 - \varrho$. The resulting inequality is (4.1). The second inequality follows from the first, after a little algebra. □

Lemma 4.2. *Let $u \in L_2(\bar{\Omega})$ and $0 < t \leq 1$. If $|\int_{\Omega_{\mathcal{I}}} u(x)dx| \leq \varepsilon|\Omega_{\mathcal{I}}|^{1/2}\|u\|_{\Omega_{\mathcal{I}}}$, with $\varepsilon \leq \frac{(1-t)\sqrt{\varrho}}{1+\sqrt{1-\varrho}}$, then*

$$\left\| u - |\bar{\Omega}|^{-1} \int_{\bar{\Omega}} u(x)dx \right\|_{\bar{\Omega}}^2 \geq \frac{t\varrho}{1 + \sqrt{1-\varrho}} \|u\|_{\bar{\Omega}}^2.$$

Proof. Note that $|\bar{\Omega}|^{-1} \int_{\bar{\Omega}} u(x)dx = \langle u, e_0 \rangle_{\bar{\Omega}} e_0$, where $e_0 = |\bar{\Omega}|^{-1/2}$ is a constant unit vector in $L_2(\bar{\Omega})$ and $\langle u, e_0 \rangle_{\bar{\Omega}} e_0$ is the orthogonal projection of u onto e_0 . Hence, $\|u - \langle u, e_0 \rangle_{\bar{\Omega}} e_0\|_{\bar{\Omega}}^2 = \|u\|_{\bar{\Omega}}^2 - |\langle u, e_0 \rangle_{\bar{\Omega}}|^2$. Since

$$\langle u, e_0 \rangle_{\bar{\Omega}} = \frac{1}{\sqrt{|\bar{\Omega}|}} \int_{\bar{\Omega}} u(x)dx,$$

we have, by Lemma 4.1, that

$$\begin{aligned} \|u - \langle u, e_0 \rangle_{\bar{\Omega}} e_0\|_{\bar{\Omega}}^2 &\geq \left(1 - \left(1 - \frac{t\varrho}{1 + \sqrt{1-\varrho}} \right)^2 \right) \|u\|_{\bar{\Omega}}^2 \\ &\geq \left(1 - \left(1 - \frac{t\varrho}{1 + \sqrt{1-\varrho}} \right) \right) \|u\|_{\bar{\Omega}}^2 = \frac{t\varrho}{1 + \sqrt{1-\varrho}} \|u\|_{\bar{\Omega}}^2. \end{aligned}$$

□

We remark that if $\int_{\Omega_{\mathcal{I}}} u(x)dx = 0$, then (4.1) becomes

$$\frac{1}{\sqrt{|\bar{\Omega}|}} \left| \int_{\bar{\Omega}} u(x)dx \right| \leq (\sqrt{1-\varrho}) \|u\|_{\bar{\Omega}},$$

and thus the lower bound in Lemma 4.2 has the form

$$\left\| u - |\overline{\Omega}|^{-1} \int_{\overline{\Omega}} u(x) dx \right\|_{\overline{\Omega}}^2 \geq \varrho \|u\|_{\overline{\Omega}}^2.$$

The point of the lemmas proved above is this. Suppose that we have a subspace Π of functions in $L_2(\Omega_{\mathcal{I}})$ with the property that $\text{dist}_{L_2(\Omega_{\mathcal{I}})}(1, \Pi) \leq \varepsilon |\Omega_{\mathcal{I}}|^{1/2}$. If we consider all $u \in L_2(\overline{\Omega})$ such that $u|_{\Omega_{\mathcal{I}}}$ is orthogonal to Π in $L_2(\Omega_{\mathcal{I}})$, then we have that, for every $p \in \Pi$,

$$\left| \int_{\Omega_{\mathcal{I}}} u dx \right| = \left| \int_{\Omega_{\mathcal{I}}} u(1-p) dx \right| \leq \|u\|_{\Omega_{\mathcal{I}}} \|1-p\|_{\Omega_{\mathcal{I}}}.$$

If we minimize over all $p \in \Pi$, then

$$(4.3) \quad \left| \int_{\Omega_{\mathcal{I}}} u dx \right| \leq \|u\|_{\Omega_{\mathcal{I}}} \text{dist}_{L_2(\Omega_{\mathcal{I}})}(1, \Pi) \leq \varepsilon |\Omega_{\mathcal{I}}|^{1/2} \|u\|_{\Omega_{\mathcal{I}}}.$$

We are now in a position to prove the lower bound for the quadratic form $a(u, u)$.

Theorem 4.3. *Suppose that $\text{dist}_{L_2(\Omega_{\mathcal{I}})}(1, \Pi) \leq \varepsilon |\Omega_{\mathcal{I}}|^{1/2}$ and that, for some $0 < t \leq 1$, $\varepsilon \leq \frac{(1-t)\sqrt{\varrho}}{1+\sqrt{1-\varrho}}$. If $\int_{\Omega_{\mathcal{I}}} u(x)p(x)dx = 0$ for all $p \in \Pi$, then*

$$(4.4) \quad a(u, u) \geq \frac{t\varrho\lambda\delta^{n+2}}{1+\sqrt{1-\varrho}} \|u\|_{\overline{\Omega}}^2,$$

where δ and λ are defined in [4, Corollary 3.4].

Proof. By [4, Corollary 3.4], which applies because γ satisfies (2.2), we have that, for all $w \in L_2(\overline{\Omega})$ such that $\int_{\overline{\Omega}} w dx = 0$, $a(w, w) \geq \lambda \delta^{n+2} \|w\|_{\overline{\Omega}}^2$. If $u \in L_2(\overline{\Omega})$, then we have $w = u - |\overline{\Omega}|^{-1} \int_{\overline{\Omega}} u(x) dx$ satisfies $\int_{\overline{\Omega}} w dx = 0$. Furthermore, for any constant c , we also have that $a(u-c, u-c) = a(u, u)$. From these facts, we thus have

$$a(u, u) \geq \lambda \delta^{n+2} \left\| u - |\overline{\Omega}|^{-1} \int_{\overline{\Omega}} u(x) dx \right\|_{\overline{\Omega}}^2.$$

The lower bound in (4.4) follows immediately from this inequality, Lemma 4.2, and (4.3). \square

Corollary 4.4. *If $\int_{\Omega_{\mathcal{I}}} u dx = 0$, then $a(u, u) \geq \frac{\varrho\lambda\delta^{n+2}}{1+\sqrt{1-\varrho}} \|u\|_{\overline{\Omega}}^2$.*

Proof. Since $\int_{\Omega_{\mathcal{I}}} u dx = 0$, Lemma 4.2 applies with $\varepsilon = 0$ and $t = 1$. The result then follows from the same argument used to prove Theorem 4.3. \square

5. LAGRANGE MULTIPLIER FORMULATION

We now want to discuss a family of variational problems that will include (2.5) and its discretizations, and these problems into Lagrange-multiplier form. We will deal with the following spaces: $U \subset L_2(\overline{\Omega})$, $\Lambda \subset L_2(\Omega_{\mathcal{I}})$, and $U^c := \{u \in U : u|_{\Omega_{\mathcal{I}}} \in \Lambda^\perp\}$. All of these are assumed to be closed.

We also assume that Λ satisfies these properties: First, let ε satisfy the conditions in Theorem 4.3. Then, we require that

$$(5.1) \quad \text{dist}_{L_2(\Omega_{\mathcal{I}})}(1, \Lambda) \leq \varepsilon |\Omega_{\mathcal{I}}|^{1/2},$$

Second, for every $\lambda \in \Lambda$ there exists an extension⁶ $\tilde{\lambda} \in U$ and a constant $\beta > 0$ such that for all $\lambda \in \Lambda$ we have

$$(5.2) \quad 0 < \beta \leq \frac{\|\lambda\|_{\Omega_{\mathcal{I}}}}{\|\tilde{\lambda}\|_{\bar{\Omega}}}.$$

Our goal is to establish the following result, which encompasses the various Lagrange multiplier problems that we wish to study.

Proposition 5.1. *There exist unique functions $u \in U$ and $\lambda \in \Lambda$ such that for all $v \in U$ and $\nu \in \Lambda$*

$$(5.3) \quad \begin{cases} a(u, v) + \int_{\Omega_{\mathcal{I}}} \lambda(x)v(x)dx = \int_{\Omega} v(x)f(x)dx, \\ \int_{\Omega_{\mathcal{I}}} u(x)\nu(x)dx = 0. \end{cases}$$

The proof will be carried out in several steps. We will begin with the following inf-sup condition for the linear functional

$$(5.4) \quad b(v, \lambda) := \int_{\Omega_{\mathcal{I}}} v(x)\lambda(x)dx, \quad v \in U \text{ and } \lambda \in \Lambda.$$

Lemma 5.2. *There exists a constant $\beta > 0$ such that*

$$(5.5) \quad \beta \leq \inf_{\lambda \in \Lambda} \sup_{v \in U} \frac{|b(v, \lambda)|}{\|v\|_{\bar{\Omega}}\|\lambda\|_{\Omega_{\mathcal{I}}}}.$$

Proof. Let λ be fixed. By the second assumption on Λ , λ has an extension $\tilde{\lambda}$ to U . Because $\tilde{\lambda} \in U$, we see that

$$\sup_{v \in U} \frac{|b(v, \lambda)|}{\|v\|_{\bar{\Omega}}\|\lambda\|_{\Omega_{\mathcal{I}}}} \geq \frac{|b(\tilde{\lambda}, \lambda)|}{\|\tilde{\lambda}\|_{\bar{\Omega}}\|\lambda\|_{\Omega_{\mathcal{I}}}} = \frac{\|\lambda\|_{\Omega_{\mathcal{I}}}^2}{\|\tilde{\lambda}\|_{\bar{\Omega}}\|\lambda\|_{\Omega_{\mathcal{I}}}} = \frac{\|\lambda\|_{\Omega_{\mathcal{I}}}}{\|\tilde{\lambda}\|_{\bar{\Omega}}} \geq \beta,$$

where the right-hand inequality follows from the assumption (5.2). Taking the infimum above yields (5.5). □

Lemma 5.3. *There exists a unique $u_0 \in U^c$ such that $a(u_0, z) = \int_{\Omega} z(x)f(x)dx$ for all $z \in U^c$.*

Proof. By Theorem 4.3 and the condition (5.1), the quadratic form $a(u, z)$ is coercive on U^c ; consequently, the Lax-Milgram theorem implies that $u_0 \in U^c$ exists and is unique. □

Proof of Proposition 5.1. With u_0 in hand, the linear functional

$$(5.6) \quad F(v) := \int_{\Omega} v(x)f(x)dx - a(u_0, v), \quad v \in U$$

satisfies $F(z) = \int_{\Omega} z(x)f(x)dx - a(u_0, z) = 0$ for all $z \in U^c$. In addition, the functional b satisfies the inf-sup condition (5.5) and is bounded on $U \otimes \Lambda$. By Lemma 10.2.12 in Brenner and Scott [7], there exists a unique $\lambda_0 \in \Lambda$ such that $b(v, \lambda_0) = F(v)$, where F is given in (5.6); that is,

$$\int_{\Omega_{\mathcal{I}}} v(x)\lambda_0(x) = \int_{\Omega} v(x)f(x)dx - a(u_0, v) \quad \forall v \in U,$$

⁶It might be thought that one can obtain $\tilde{\lambda}$ by simply taking $\tilde{\lambda} = 0$ on Ω . But since we require $\tilde{\lambda} \in U$, this will not work in general; however, it will work if $U = L_2(\Omega_{\mathcal{I}})$. See Section 5.1.

so the first equation in (5.3) holds. The second is a consequence u_0 being in U^c . Making the replacements $u_0 \rightarrow u$ and $\lambda_0 \rightarrow \lambda$ completes the proof. \square

5.1. The continuous case with Dirichlet volume constraint. We now turn to the problem of solving $a(u, v) = \int_{\Omega} v(x)f(x)dx$, with $u, v = 0$ a.e. on $\Omega_{\mathcal{I}}$. Consider the following spaces: $U = L_2(\overline{\Omega})$, $\Lambda = L_2(\Omega_{\mathcal{I}})$, and $U^c := L_2^c(\overline{\Omega}) = \{u \in L_2(\overline{\Omega}) : u|_{\Omega_{\mathcal{I}}} = 0 \text{ a.e.}\}$. We want to cast this problem into the form (5.3).

Theorem 5.4. *Let U , Λ and U^c be as above. Then there exist unique functions $u \in U^c$ and $\lambda \in \Lambda$ that solve (5.3).*

Proof. We begin by noting that $a(u, v)$ is coercive on U^c . This follows from Corollary 4.4, since all functions in U^c are 0 on \mathcal{I} , they are obviously orthogonal to $\text{span}\{1\}$ on $\Omega_{\mathcal{I}}$. Moreover, if $\lambda \in \Lambda = L_2(\Omega_{\mathcal{I}})$, then we may define its extension to $U = L_2(\overline{\Omega})$ by simply setting $\tilde{\lambda}|_{\Omega} = 0$. Hence, $\|\tilde{\lambda}\|_{\overline{\Omega}} = \|\lambda\|_{\Omega_{\mathcal{I}}}$, and Λ satisfies the condition (5.2), with $\beta = 1$. Finally, the condition (5.1) is satisfied, since $1|_{\Omega_{\mathcal{I}}} \in L_2(\Omega_{\mathcal{I}})$ implies that (5.1) holds with $\varepsilon = 0$. \square

There is an integral-equation approach to this problem. Let λ and u be the solutions to the Lagrange equations found above. We start by showing that λ is given by an integral operator applied to u , and then use this fact to obtain a Fredholm equation for u . The assertion concerning λ is proved below.

Lemma 5.5. *For $\nu \in L_2(\Omega_{\mathcal{I}})$, let $\tilde{\nu}$ be the extension by 0 of ν to $L_2(\overline{\Omega})$. If $\int_{\Omega_{\mathcal{I}}} \lambda(x)\nu(x)dx = -a(u, \tilde{\nu}) \forall \nu \in L_2(\Omega_{\mathcal{I}})$, then $\lambda(x) = 2 \int_{\Omega} \gamma(x, y)u(y)dy$, $x \in \Omega_{\mathcal{I}}$.*

Proof. The support of $u \in U^c$ is Ω . Because $\tilde{\nu} = 0$ on Ω , its support is $\Omega_{\mathcal{I}}$. Thus $u(x)\tilde{\nu}(x) = 0$ for all $x \in \overline{\Omega}$. This and the symmetry of γ then imply that $a(u, \tilde{\nu}) = -2 \int_{\overline{\Omega}} \int_{\overline{\Omega}} \gamma(x, y)\tilde{\nu}(x)u(y)dydx$. Using the supports of u and $\tilde{\nu}$ in the previous expression yields

$$(5.7) \quad a(u, \tilde{\nu}) = \int_{\Omega_{\mathcal{I}}} \left(-2 \int_{\Omega} \gamma(x, y)u(y)dy \right) \nu(x)dx,$$

since $\tilde{\nu}|_{\Omega_{\mathcal{I}}} = \nu$. By assumption, we have

$$\int_{\Omega_{\mathcal{I}}} \nu(x)\lambda(x)dx = \int_{\Omega_{\mathcal{I}}} \left(2 \int_{\Omega} \gamma(x, y)u(y)dy \right) \nu(x)dx,$$

which holds for all $\nu \in L_2(\Omega_{\mathcal{I}})$. Comparing the two sides yields the desired formula for λ . \square

Silling [22, p. 98, eq. 37] derives a Fredholm equation of the second kind for a generalization of the type of equilibrium problem we are dealing with here. In our case, the integral equation is the following:

$$(5.8) \quad \sigma(x)u(x) - \int_{\Omega} \gamma(x, y)u(y)dy = \frac{1}{2}f(x), \quad \sigma(x) = \int_{\overline{\Omega}} \gamma(x, y)dy, \quad x \in \Omega.$$

The next two results discuss this equation. We begin with the properties of σ .

Lemma 5.6. *Let $B_{\delta} := \{(x, y) \in \overline{\Omega} \times \overline{\Omega} : |x - y| \leq \delta\}$, $\delta > 0$. Suppose that there are positive constants δ, c_0 for which $c_0 \leq \gamma(x, y)$ for all $(x, y) \in B_{\delta}$. Then, $\sigma(x) \geq c_0\omega_{n-1}\delta^n/n$, where ω_{n-1} is the volume of \mathbb{S}^{n-1} .*

Proof. We may assume that $\delta < \text{dist}(\Omega, \overline{\Omega}^c)$. For fixed $x \in \Omega$, the ball centered at x with radius δ will be in B_δ . Hence, again for fixed $x \in \Omega$, $\gamma(x, y) \geq c_0$, and so $\sigma(x) \geq c_0 \int_{|x-y| \leq \delta} dy = \omega_n c_0 \delta^n / n$. \square

This lemma allows us to divide by σ , take its square root, and so on. Carrying out such manipulations allows us to put the Fredholm equation (5.8) in the form given below.

Proposition 5.7. *With the assumptions made in Lemma 5.6, we have*

$$(5.9) \quad u(x) - \int_{\Omega} \frac{\gamma(x, y)}{\sigma(x)} u(y) dy = \frac{f(x)}{2\sigma(x)}, \quad x \in \Omega.$$

In addition, if we let $w(x) := \sqrt{\sigma(x)}u(x)$ and $\tilde{\gamma}(x, y) = \gamma(x, y)/\sqrt{\sigma(x)\sigma(y)}$, then (5.8) has the self-adjoint form

$$(5.10) \quad w(x) - \int_{\Omega} \tilde{\gamma}(x, y)w(y) dy = \frac{f(x)}{\sqrt{2\sigma(x)}}, \quad x \in \Omega.$$

For future reference, we point out that when $\gamma(x, y) = \gamma(|x - y|)$ the function $\sigma(x)$ will be constant in Ω . To see this, suppose that the support of $\gamma(r)$ is $[0, \delta]$, where we assume that $\delta < \text{dist}(\Omega, \overline{\Omega}^c)$. Fix $x \in \Omega$, the ball $|x - y| \leq \delta$ is then contained in $\overline{\Omega}$. Thus,

$$\sigma(x) = \int_{\overline{\Omega}} \gamma(|x - y|) dy = \int_{|x-y| \leq \delta} \gamma(|x - y|) dy = \omega_{n-1} \int_0^\delta \gamma(r)r^{n-1} dr := \sigma_\gamma.$$

The right side is independent of x , so $\sigma(x) = \sigma_\gamma$ is constant on $\overline{\Omega}$. In fact, it is constant for all $x \in \overline{\Omega}$ for which the ball $|x - y| \leq \delta$ is contained in $\overline{\Omega}$.

5.2. The discrete case. Discretizing the problem begins with choosing a basis of functions to work with. For us, this will be a set of local Lagrange functions associated with a positive definite or conditionally positive definite RBF kernel and a set of centers⁷ X in $\overline{\Omega}$. We will denote the basis by $B = \{b_\xi : \xi \in X\}$. We will use B to construct the three spaces U_h , U_h^c , and Λ_h . As usual, h refers to a mesh norm. We assume that, on Ω , $\Omega_{\mathcal{I}}$, and $\overline{\Omega}$, the distribution of centers is quasi-uniform. These three spaces are defined this way: $U_h = \text{span}\{b_\xi : \xi \in X\}$, $\Lambda_h := \text{span}\{b_\xi|_{\Omega_{\mathcal{I}}} : \xi \in X \cap \Omega_{\mathcal{I}}\}$, and $U_h^c = \{u \in U_h : u|_{\Omega_{\mathcal{I}}} \in \Lambda_h^\perp\}$.

We now need to discuss conditions (5.1) and (5.2) in connection with Λ_h . Because RBFs have excellent approximation power, getting $\text{dist}_{L_2(\Omega_{\mathcal{I}})}(1|_{\Omega_{\mathcal{I}}}, \Lambda_h)$ to satisfy the bound in Theorem 4.3 for any ε only requires taking h sufficiently small and the K in $r_h = Kh|\log(h)|$, sufficiently large. Our next result proves this, along with a coercivity result.

Lemma 5.8. *Let ϱ , ε and t be as in Theorem 4.3 and let $\Lambda_h := \text{span}\{b_\xi|_{\Omega_{\mathcal{I}}} : \xi \in X \cap \Omega_{\mathcal{I}}\}$ be as in (2.7), with $\psi_k \rightarrow b_\xi$. Then, for h sufficiently small and K sufficiently large, we have that*

$$(5.11) \quad \text{dist}_{L_2(\Omega_{\mathcal{I}})}(1|_{\Omega_{\mathcal{I}}}, \Lambda_h) \leq \varepsilon |\Omega_{\mathcal{I}}|^{1/2}.$$

⁷To construct the Lagrange functions, we will make use of a slightly larger set of centers, $Y \supset X$. The centers in $Y \setminus X$ will be outside of $\overline{\Omega}$.

In addition, if $u_h \in U_h^c$, then

$$(5.12) \quad a(u_h, u_h) \geq \frac{t\rho\lambda\delta^{d+2}}{1 + \sqrt{1 - \rho}} \|u_h\|_{\bar{\Omega}}^2.$$

Proof. Choose $\alpha > 0$ so that the set $\Omega_{\mathcal{I}}^\varepsilon := \{x \in \Omega_{\mathcal{I}} : \text{dist}(x, \partial\Omega_{\mathcal{I}}) \leq \alpha\varepsilon\}$ has volume $|\Omega_{\mathcal{I}}^\varepsilon| \leq \frac{1}{4}\varepsilon^2|\Omega_{\mathcal{I}}|$. Let $\psi_\varepsilon : \Omega_{\mathcal{I}} \rightarrow [0, 1]$ be a compactly supported C^∞ function for which $\psi_\varepsilon = 1$ on the set $\Omega_{\mathcal{I}} \setminus \Omega_{\mathcal{I}}^\varepsilon$. Next, form the quasi-interpolant $s_h := \tilde{I}_{X \cap \Omega_{\mathcal{I}}} \psi_\varepsilon \in V_h$. Applying Theorem 3.5, we have that

$$\|\psi_\varepsilon - s_h\|_{L_2(\Omega_{\mathcal{I}})} \leq Ch^2 \|\psi_\varepsilon\|_{W_2^2(\Omega_{\mathcal{I}})}$$

for all h sufficiently small and K sufficiently large. Since ε is fixed and h and K are at our disposal, we may also choose them so that

$$Ch^2 \|\psi_\varepsilon\|_{W_2^2(\Omega_{\mathcal{I}})} \leq \frac{\varepsilon}{2} |\Omega_{\mathcal{I}}|^{1/2}.$$

Finally, we note that $\|1|_{\Omega_{\mathcal{I}}} - s_h\|_{L_2(\Omega_{\mathcal{I}})} \leq \|1|_{\Omega_{\mathcal{I}}} - \psi_\varepsilon\|_{L_2(\Omega_{\mathcal{I}})} + \|\psi_\varepsilon - s_h\|_{L_2(\Omega_{\mathcal{I}})}$. Because $\psi_\varepsilon = 1$ on $\Omega_{\mathcal{I}} \setminus \Omega_{\mathcal{I}}^\varepsilon$, we have that $\|1|_{\Omega_{\mathcal{I}}} - \psi_\varepsilon\|_{L_2(\Omega_{\mathcal{I}})} = \|1|_{\Omega_{\mathcal{I}}} - \psi_\varepsilon\|_{L_2(\Omega_{\mathcal{I}}^\varepsilon)} \leq \|1|_{\Omega_{\mathcal{I}}}\|_{L_2(\Omega_{\mathcal{I}}^\varepsilon)} \leq \frac{\varepsilon}{2} |\Omega_{\mathcal{I}}|^{1/2}$. Hence, $\|1|_{\Omega_{\mathcal{I}}} - s_h\|_{L_2(\Omega_{\mathcal{I}})} \leq \frac{\varepsilon}{2} |\Omega_{\mathcal{I}}|^{1/2} + \frac{\varepsilon}{2} |\Omega_{\mathcal{I}}|^{1/2} = \varepsilon |\Omega_{\mathcal{I}}|^{1/2}$. The coercivity result (5.12) now follows directly from Theorem 4.3. \square

Note that the lower bound in (5.12) is independent of h , as long as h is sufficiently small; i.e., $h \leq h_0$. This is very important for the method we will use in approximating u by u_h . To proceed further, we also need to show that Λ_h satisfies the condition in (5.2).

Lemma 5.9 (Discrete inf-sup condition). *Consider $\lambda = \sum_{\xi \in X \cap \Omega_{\mathcal{I}}} c_\xi b_\xi|_{\Omega_{\mathcal{I}}} \in \Lambda_h$ and let $\tilde{\lambda} := \sum_{\xi \in X \cap \Omega_{\mathcal{I}}} c_\xi b_\xi$, which is an extension of λ to U_h . Then, there exist constants $\beta > 0$ and $h_0 > 0$, which are independent of λ , such that $\beta \|\tilde{\lambda}\|_{\bar{\Omega}} \leq \|\lambda\|_{\Omega_{\mathcal{I}}}$ holds for all $h \leq h_0$.*

Proof. From [14, Theorem 4.11] for h sufficiently small, we have

$$\|\tilde{\lambda}\|_{\bar{\Omega}} \leq Ch^{n/2} \|(c_\xi)_{\xi \in X \cap \Omega_{\mathcal{I}}}\|_{\ell_2}.$$

We will now make use of [14, Proposition 4.12]. Replace Ω in the proposition by $\Omega_{\mathcal{I}}$, s by λ , and q by h/ρ . Then, we have that

$$c \|(c_\xi)_{\xi \in X \cap \Omega_{\mathcal{I}}}\|_{\ell_2} \leq \rho^{n/2} h^{-n/2} \|\lambda\|_{\Omega_{\mathcal{I}}}.$$

Let $\beta = (C\rho^{n/2})^{-1}$. Combining the inequalities then gives $\beta \|\tilde{\lambda}\|_{\bar{\Omega}} \leq \|\lambda\|_{\Omega_{\mathcal{I}}}$. \square

Theorem 5.10. *Let U_h , Λ_h , h_0 and U_h^c be defined as above. For all $h \leq h_0$, there exist unique functions $u_h \in U_h^c$ and $\lambda_h \in \Lambda_h$ such that for all $v_h \in U_h$ and $\nu_h \in \Lambda_h$ the following discretized version of (2.6) holds:*

$$(5.13) \quad \begin{cases} a(u_h, v_h) + \int_{\Omega_{\mathcal{I}}} \lambda_h(x) v_h(x) dx = \int_{\Omega} v_h(x) f(x) dx, \\ \int_{\Omega_{\mathcal{I}}} u_h(x) \nu_h(x) dx = 0. \end{cases}$$

Proof. Putting together Lemma 5.8, Lemma 5.9 and Proposition 5.1 yields the result. \square

5.3. Error Estimates. To get error estimates, we will apply results found in Sections 10.3 and 10.5 of Brenner and Scott [7], which (in our notation) make the assumption that $U_h \subset U = L_2(\overline{\Omega})$ and $\Lambda_h \subset \Lambda = L_2(\Omega_{\mathcal{I}})$. These results hold here because the local Lagrange basis $B = \{b_\xi : \xi \in X\}$ is in $U = L_2(\overline{\Omega})$; and also, the restrictions of them to $\Omega_{\mathcal{I}}$ are in $\Lambda = L_2(\Omega_{\mathcal{I}})$. We can now obtain error estimates for the case at hand.

Theorem 5.11. *Adopt the notation and assumptions made in Sections 5.1 and 5.2. Then, for $h \leq h_0$,*

$$\|u - u_h\|_{\overline{\Omega}} + \|\lambda - \lambda_h\|_{\Omega_{\mathcal{I}}} \leq C(\text{dist}_{L_2(\overline{\Omega})}(u, U_h) + \text{dist}_{L_2(\Omega_{\mathcal{I}})}(\lambda, \Lambda_h)).$$

Proof. We want to apply [7, Corollary 10.5.18]. There are three ingredients needed. In order, the boundedness of $a(u, v), b(v, \lambda)$, the coercivity of $a(u, v)$, and a discrete inf-sup condition for $b(v, \lambda)$. The first of these is obvious from the definition of $a(u, v)$, given in (2.4), and of $b(v, \lambda)$, given in (5.4). The second, the coercivity of a , follows from Corollary 4.4 in the continuous case, and Lemma 5.8 in the discrete case. Finally, the discrete inf-sup condition was established in Lemma 5.9. It follows that [7, Corollary 10.5.18] implies the desired error estimate. \square

At this point getting rates of convergence will depend on two factors: (1) the smoothness of u and λ ; and, (2) the RBF used in the problem. The discussion concerning the Fredholm approach in Section 5.1 provides an approach to finding the smoothness of u and λ . If that can be done, it will be possible to get rates.

The situations for u and λ are different. Since $u|_{\Omega_{\mathcal{I}}} = 0$, the solution u is compactly supported in $\overline{\Omega}$ and thus, by Theorem 3.5, the error rates depend only on the smoothness of the kernel $\gamma(x, y)$ and on the source f . If these yield $u \in W_2^\beta(\overline{\Omega})$, then distance estimate in (3.26) implies that

$$(5.14) \quad \text{dist}_{L_2(\overline{\Omega})}(u, U_h) \leq Ch^\beta \|u\|_{W_2^\beta(\overline{\Omega})}.$$

It may also be possible that u turns out to be in W_2^{2m} , then, in view of Remark 3.6, we expect that the error rates should double; i.e., h^{2m} rather than h^m . This is born out by the numerical results shown in Figure 2. The expected rate would be about h^2 , but the rate we obtained is $h^{3.3}$. (It's lower than h^4 because u is not quite in W_2^4 .)

For λ , the smoothness is known. From Lemma 5.5, we have that $\lambda(x) = 2 \int_{\Omega} \gamma(x, y)u(y)dy, x \in \Omega_{\mathcal{I}}$. This formula obviously holds for all $x \in \overline{\Omega}$ and thus extends λ to $\overline{\Omega}$. Differentiating under the integral sign implies that the extension of λ to $\overline{\Omega}$ is as smooth as $\gamma(x, y)$.

We also have information about the support of λ . Since $\gamma(x, y) = 0$ for $|x - y| \geq \delta > 0$, the Lagrange multiplier $\lambda(x) = 0$ when $\text{dist}(x \in \Omega_{\mathcal{I}}, \Omega) \geq \delta$. Consequently, λ is compactly supported in $\overline{\Omega}$.

Unfortunately, this isn't sufficient to apply Theorem 3.5 *as stated*. To be able to do that, λ must be compactly supported *in* $\Omega_{\mathcal{I}}$. The reason is that the local Lagrange functions employed use only centers in $X \cap \Omega_{\mathcal{I}}$, rather than all of X . Even so, as we conjectured in Remark 3.6, we expect the to see rates at least those given in Theorem 3.5 to hold. The numerics again bear this out.

6. NUMERICAL RESULTS

We present numerical results for experiments using the discretization described in Section 2 and analyzed in Sections 5.2 and 5.3. The numerical method requires a preprocessing step for constructing the basis, a step of assembling and solving the linear system that arises from the Galerkin method discussed in Sections 5.2., and then a post-processing step for evaluating the L^2 error. We discuss the computational methods we employ for each step. The resulting experiments validate the L^2 error estimates derived in Section 3.2.

We consider solving two-dimensional versions of the problems discussed in Section 5.2, with a radial kernel Φ and two different diffusion coefficients κ ; see Sections 6.1 and 6.2. For each experiment, we test with zero Dirichlet volume constraints although no noticeable difference occurs in the non-zero Dirichlet volume constraint case. The domain of interest for the experiments is denoted $\Omega \cup \Omega_I$ where $\Omega = (0, 1) \times (0, 1)$ and $\Omega_I = [-\frac{1}{4}, \frac{5}{4}] \times [-\frac{1}{4}, \frac{5}{4}] \setminus \Omega$ denote the volume constraint region or interaction domain. MATLAB is used for the experiments and plots. Experimental results presented here are the result of directly using the MATLAB backslash operator, which solves the linear set of equations using a sparse direct method.

The local Lagrange functions are constructed with linear combinations of the thin plate spline $r^2 \log(r)$. Each local Lagrange function is constructed using approximately $11(\log N)^2$ nearest neighbor centers, where N is the total number of centers in $\Omega \cup \Omega_I$. The local Lagrange functions are constructed as discussed in Section 3.3.

For each numerical experiment, we choose a kernel γ , an anisotropy term κ , and a function $u \in L^2_c(\Omega \cup \Omega_I)$; i.e., u satisfies the volume constraint. The source function f is manufactured by computing $\mathcal{L}u(x_i) = f(x_i)$ for each center x_i , where

$$(6.1) \quad \mathcal{L}u(x) := \int_{\Omega} (u(x) - u(y)) (\kappa(x) + \kappa(y)) \Phi(\|x - y\|) dy$$

is the strong form corresponding to the bilinear form (2.4). We express the kernel γ from (2.4) as $\gamma(x, y) := \frac{1}{2}(\kappa(x) + \kappa(y))\Phi(\|x - y\|)$.

The values of $f(x_i)$ are computed by using tensor products of Gauss-Legendre quadrature nodes to approximate the integral in (6.1).

We study L^2 convergence of the discrete solution by constructing sets of uniformly spaced centers with various mesh norms. Uniformly spaced collections of centers X_h are constructed using grid spacing $h = .04, .02, .014$, and $.006$. The convergence of the discrete solution u_h to the solution u is measured by plotting the L^2 norm of the error $\|u_h - u\|_{L^2(\Omega \cup \Omega_I)}$ against the mesh norm h . The error is computed by using tensor products of Gauss-Legendre quadrature nodes over the grid $\tilde{\Omega}$.

6.1. Linear diffusion coefficient. We choose u , κ and the radial function Φ to be

$$(6.2) \quad \begin{cases} u(x_1, x_2) = (x_1(1 - x_1))^{\frac{3}{2}}(x_2(1 - x_2))^{\frac{3}{2}} \mathbb{1}_{\Omega}(x_1, x_2), \\ \kappa(x_1, x_2) = 1 + x_1 + x_2, \\ \Phi_{\varepsilon}(\|x - y\|) = \exp(- (1 - \varepsilon^{-2}\|x - y\|^2)^{-1}), \end{cases}$$

and thus $\gamma(x, y) := \frac{1}{2}(\kappa(x) + \kappa(y))\Phi(\|x - y\|)$, with $x = (x_1, x_2)$ and $y = (y_1, y_2)$.

TABLE 1. The mesh norm h , number of rows n of the stiffness matrix, and the estimated condition number for the stiffness matrix with the linear diffusion coefficient (6.2) and the exponential diffusion coefficient (6.3). The condition numbers of the stiffness matrices do not increase as h decreases.

Approximate Condition Number			
h	n	Linear	Exponential
2.83e-2	1444	207	227
1.41e-2	5776	171	222
9.9e-3	11449	170	219
5.7e-3	35344	179	223

Figure 1 displays the observed L^2 convergence rates with respect to the mesh norm h . The log of the computed L^2 error versus the log of the mesh norm is presented along with a best fit line to estimate the convergence order of the observed data. The smooth solution exhibits a convergence rate of approximately h^3 .

We mention that in this experiment the $J(\xi)$'s in (3.29) were computed numerically using the tensor-product Gauss-Legendre method. The experiment was also done with exact $J(\xi)$'s calculated analytically using the method in Appendix A. The results were virtually the same.

Table 1 displays the condition numbers of the discrete stiffness matrices. The observed condition numbers of the stiffness matrices do not increase as the mesh norm decreases, which suggests that for quasi-uniformly distributed centers, the condition number of the stiffness matrix and the mesh norm h are independent. This prediction is supported by a similar result for the case of a conforming local Lagrange method [16].

6.2. Exponential diffusion coefficient. For this experiment, we use the functions u , κ and Φ given by

$$(6.3) \quad \begin{cases} u(x_1, x_2) = \sin(2\pi x_1) \sin(2\pi x_2) \mathbb{1}_\Omega(x_1, x_2), \\ \kappa(x_1, x_2) = \exp(x_1 + x_2), \\ \Phi_\varepsilon(\|x - y\|) = \exp(- (1 - \varepsilon^{-2}\|x - y\|^2)^{-1}). \end{cases}$$

Again, $\gamma(x, y) := \frac{1}{2}(\kappa(x) + \kappa(y))\Phi(\|x - y\|)$, with $x = (x_1, x_2)$ and $y = (y_1, y_2)$.

Figure 2 displays the L^2 convergence plots for the experiments involving u_2 and κ_2 . The solution u is not continuously differentiable, so we expect a convergence rate of at most h^2 . A convergence rate of $h^{1.88}$ is observed. In this experiment the exact $J(\xi)$'s in (3.29) were analytically determined via the method in Appendix A. The experiment was also done with numerically computed $J(\xi)$'s. The analytical method gave a convergence rate about 0.1 higher than the numerical method.

APPENDIX A

In this section we will compute the integrals for the $J(\xi)$'s defined in (3.29). We will begin by translating D to $D + \xi$, so that in the new coordinates ξ is at the origin and $J(\xi)$ has the form

$$J(\xi) = \int_{D+\xi} \phi(|x|) dx dy.$$

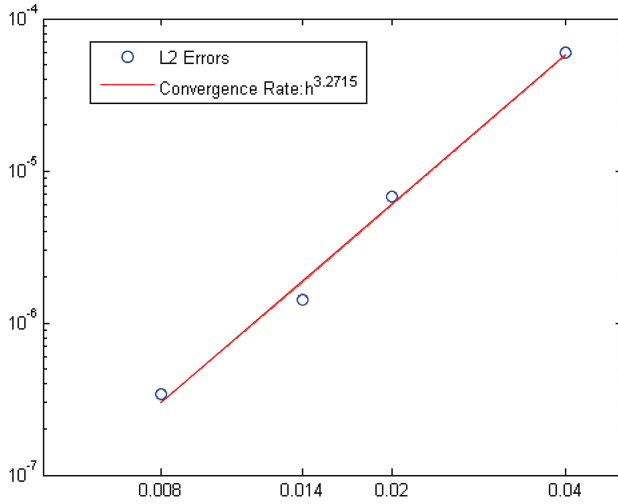


FIGURE 1. The log of h versus the log of the L^2 error for the linear diffusion coefficient experiment with functions given by (6.2) is displayed.

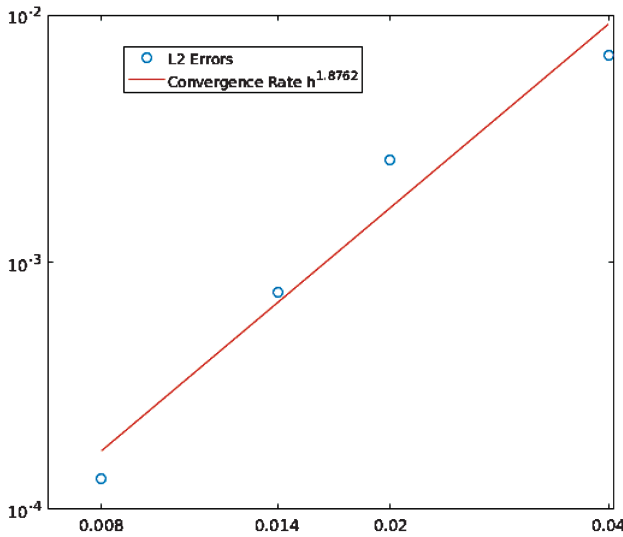


FIGURE 2. The log of h versus the log of the L^2 error for the exponential diffusion coefficient experiment with functions given by (6.3) is displayed.

To simplify notation, we will use D rather than $D + \xi$, inserting the latter at the end of the calculations.

Suppose that $\phi(|x|)$ satisfies an equation of the form $\Delta\Phi(|x|) = \phi(|x|)$. For example, when $\phi(r) = \phi_2(r) = r^2 \log(r)$, we have $\Phi(r) = \frac{r^4}{32}(2 \log(r) - 1)$, where $r = |x|$. When this happens, we may employ Green's theorem to obtain the following

formula:

$$J(\xi) = \int_D \phi(|x|) dx dy = \int_D \Delta\Phi(|x|) dx dy = \oint_{\partial D} \hat{\mathbf{n}} \cdot \nabla\Phi(|x(s)|) ds,$$

or equivalently,

$$(A.1) \quad J(\xi) = \oint_{\partial D} -\frac{\partial\Phi(|x|)}{\partial y} dx + \frac{\partial\Phi(|x|)}{\partial x} dy, \quad |x| = \sqrt{x^2 + y^2}.$$

Since

$$\frac{\partial\Phi(|x|)}{\partial x} = \frac{x}{|x|} \Phi'(|x|) \text{ and } \frac{\partial\Phi(|x|)}{\partial y} = \frac{y}{|x|} \Phi'(|x|),$$

we have

$$(A.2) \quad J(\xi) = \oint_{\partial D} \frac{\Phi'(|x|)}{|x|} (-y dx + x dy).$$

It follows that instead of using a 2D quadrature rule, one can get away with a 1D rule. Even better, in the case where $\phi(r) = r^2 \log(r)$ and D is a polygonal domain, these integrals can be computed analytically.

We begin by observing that

$$\frac{\Phi'(r)}{r} = \frac{r^2}{16} (2 \log(r^2) - 1),$$

consequently,

$$J(\xi) = \oint_{\partial D} \frac{r^2}{16} (2 \log(r^2) - 1) (-y dx + x dy).$$

If D is a *polygonal* domain, the boundary ∂D consists of a chain of directed line segments. A typical line segment L starts at (a, A) and ends at (b, B) . Let $\mathbf{a} := a\mathbf{i} + A\mathbf{j}$, $\mathbf{b} = b\mathbf{i} + B\mathbf{j}$ and $\boldsymbol{\delta} := \mathbf{b} - \mathbf{a}$. Parametrize L by $\mathbf{x} = \mathbf{a} + t\boldsymbol{\delta}$, $0 \leq t \leq 1$. It is easy to show that $-y dx + x dy = (aB - bA) dt = (\mathbf{k} \cdot \mathbf{a} \times \boldsymbol{\delta}) dt$. In addition, we have that

(A.3)

$$r^2 = |\mathbf{a} + t\boldsymbol{\delta}|^2 = \alpha^2 + z^2, \text{ where } z = |\boldsymbol{\delta}|t + \frac{\mathbf{a} \cdot \boldsymbol{\delta}}{|\boldsymbol{\delta}|}, \quad \alpha := \pm \sqrt{|\mathbf{a}|^2 - \frac{(\mathbf{a} \cdot \boldsymbol{\delta})^2}{|\boldsymbol{\delta}|^2}} = \frac{\mathbf{a} \times \boldsymbol{\delta} \cdot \mathbf{k}}{|\boldsymbol{\delta}|}.$$

Thus the line integral over L may be put in the form

$$\int_L \frac{r^2}{16} (2 \log(r^2) - 1) (-y dx + x dy) = \alpha \int_{\frac{\mathbf{a} \cdot \boldsymbol{\delta}}{|\boldsymbol{\delta}|}}^{\frac{\mathbf{b} \cdot \boldsymbol{\delta}}{|\boldsymbol{\delta}|}} \frac{\alpha^2 + z^2}{16} (2 \log(\alpha^2 + z^2) - 1) dz.$$

It follows that we need to compute two indefinite integrals. First, we have

$$\begin{aligned} \int (z^2 + \alpha^2) \log(z^2 + \alpha^2) dz &= \int \log(z^2 + \alpha^2) d\left(\frac{1}{3}(z^3 + 3\alpha^2 z)\right) \\ &= \frac{1}{9}(z^3 + 3\alpha^2 z)(3 \log(z^2 + \alpha^2) - 2) + \frac{4\alpha^2}{3} \tan^{-1}(z/\alpha) - \frac{2\alpha^2}{3} z. \end{aligned}$$

Second, $\int (z^2 + \alpha^2) dz = \frac{1}{3}(z^3 + 3\alpha^2 z)$. Combining this result with the previous integral yields

$$\begin{aligned} &\alpha \int \frac{\alpha^2 + z^2}{16} (2 \log(\alpha^2 + z^2) - 1) dz \\ &= \frac{\alpha z^3 + 3\alpha^3 z}{144} (6 \log(z^2 + \alpha^2) - 7) + \frac{\alpha^4}{6} \tan^{-1}(z/\alpha) - \frac{\alpha^3}{12} z =: f(z, \alpha). \end{aligned}$$

Finally, we arrive at the integral over the line segment L :

$$(A.4) \quad \int_L \frac{r^2}{16} (2 \log(r^2) - 1) (-y dx + x dy) = f\left(\frac{\mathbf{b} \cdot \hat{\boldsymbol{\delta}}}{|\hat{\boldsymbol{\delta}}|}, \alpha\right) - f\left(\frac{\mathbf{a} \cdot \hat{\boldsymbol{\delta}}}{|\hat{\boldsymbol{\delta}}|}, \alpha\right),$$

where α is defined in (A.3).

We can give a geometric interpretation to the parameters involved. Let $\hat{\boldsymbol{\delta}} = \boldsymbol{\delta}/|\boldsymbol{\delta}|$. Then $\alpha = \mathbf{a} \times \hat{\boldsymbol{\delta}} \cdot \mathbf{k}$ is the (signed) area of the parallelogram with sides \mathbf{a} and $\hat{\boldsymbol{\delta}}$. The endpoints $\mathbf{a} \cdot \hat{\boldsymbol{\delta}}$ and $\mathbf{b} \cdot \hat{\boldsymbol{\delta}}$ are, respectively, projections of \mathbf{a} and \mathbf{b} onto $\boldsymbol{\delta}$.

Restoring ξ to the problem means replacing D above by $D + \xi$, and L by $L + \xi$. The effect on the integrals is to change \mathbf{a} and \mathbf{b} to $\mathbf{a} + \xi$ and $\mathbf{b} + \xi$. Of course, $\boldsymbol{\delta}$ remains the same. There is one more step. To get back to the original problem, namely calculating $J(\xi) = \int_D \phi(x - \xi) dx$, observe that in a line segment L_{orig} starting at \mathbf{a}_{orig} and ending at \mathbf{b}_{orig} , the endpoints are related to those of $L_{\text{orig}} + \xi$ via $\mathbf{a}_{\text{orig}} = \mathbf{a} + \xi$ and $\mathbf{b}_{\text{orig}} = \mathbf{b} + \xi$. Thus, in the equations above one should use

$$\begin{aligned} \mathbf{a} &= \mathbf{a}_{\text{orig}} - \xi \quad \text{and} \quad \mathbf{b} = \mathbf{b}_{\text{orig}} - \xi, \\ \boldsymbol{\delta} &= \mathbf{b}_{\text{orig}} - \mathbf{a}_{\text{orig}}, \\ \alpha &= \frac{(\mathbf{a}_{\text{orig}} - \xi) \times \boldsymbol{\delta} \cdot \mathbf{k}}{|\boldsymbol{\delta}|}. \end{aligned}$$

We conclude by pointing out that the same argument may be used to compute $J(\xi)$ for any TPS $\phi_m(r) = r^{2m} \log(r)$, $m \geq 1$. Specifically, it is easy to show that

$$\Phi_m(r) := \frac{1}{4(m+1)^3} ((m+1)\phi_{m+1}(r) - r^{2m+2})$$

satisfies $\Delta \Phi_m = \phi_m$. Although more complicated, the same integration-by-parts trick still works and will allow us to evaluate $J(\xi)$ exactly.

ACKNOWLEDGMENTS

The authors wish to thank both anonymous referees for a very careful reading of the manuscript. In particular, we wish to thank one of the referees for pointing out the paper [15]. We also wish to acknowledge the Texas A&M University Brazos HPC cluster [1], which contributed to the research reported here.

REFERENCES

- [1] Academy for Advanced Telecommunications and Learning Technologies, *Texas A&M University Brazos HPC*, <http://brazos.tamu.edu>, 2015.
- [2] G. Acosta and J. P. Borthagaray, *A fractional Laplace equation: regularity of solutions and finite element approximations*, SIAM J. Numer. Anal. **55** (2017), no. 2, 472–495, DOI 10.1137/15M1033952. MR3620141
- [3] R. A. Adams, *Sobolev Spaces*, Academic Press [A subsidiary of Harcourt Brace Jovanovich, Publishers], New York-London, 1975. Pure and Applied Mathematics, Vol. 65. MR0450957
- [4] B. Aksoylu and T. Mengesha, *Results on nonlocal boundary value problems*, Numer. Funct. Anal. Optim. **31** (2010), no. 12, 1301–1317, DOI 10.1080/01630563.2010.519136. MR2738853
- [5] I. Babuška, U. Banerjee, and J. E. Osborn, *Survey of meshless and generalized finite element methods: a unified approach*, Acta Numer. **12** (2003), 1–125, DOI 10.1017/S0962492902000090. MR2249154
- [6] S. D. Bond, R. B. Lehoucq, and S. T. Rowe, *A Galerkin radial basis function method for non-local diffusion*, Meshfree methods for partial differential equations VII, Lect. Notes Comput. Sci. Eng., vol. 100, Springer, Cham, 2015, pp. 1–21. MR3587375
- [7] S. C. Brenner and L. R. Scott, *The mathematical theory of finite element methods*, 3rd ed., Texts in Applied Mathematics, vol. 15, Springer, New York, 2008. MR2373954

- [8] N. Burch, M. D’Elia, and R.B. Lehoucq, *The exit-time problem for a Markov jump process*, The European Physical Journal Special Topics **223** (2014), no. 14, 3257–3271.
- [9] M. D’Elia and M. Gunzburger, *The fractional Laplacian operator on bounded domains as a special case of the nonlocal diffusion operator*, Comput. Math. Appl. **66** (2013), no. 7, 1245–1260, DOI 10.1016/j.camwa.2013.07.022. MR3096457
- [10] Q. Du, M. Gunzburger, R. B. Lehoucq, and K. Zhou, *Analysis and approximation of nonlocal diffusion problems with volume constraints*, SIAM Rev. **54** (2012), no. 4, 667–696, DOI 10.1137/110833294. MR3023366
- [11] G. E. Fasshauer, *Meshfree Approximation Methods with MATLAB*, Interdisciplinary Mathematical Sciences, vol. 6, World Scientific Publishing Co. Pte. Ltd., Hackensack, NJ, 2007. MR2357267
- [12] E. Fuselier, T. Hangelbroek, F. J. Narcowich, J. D. Ward, and G. B. Wright, *Localized bases for kernel spaces on the unit sphere*, SIAM J. Numer. Anal. **51** (2013), no. 5, 2538–2562, DOI 10.1137/120876940. MR3097032
- [13] T. Hangelbroek, *On local RBF approximation*, Adv. Comput. Math. **37** (2012), no. 2, 285–299, DOI 10.1007/s10444-011-9212-5. MR2944053
- [14] Thomas Hangelbroek, Francis J. Narcowich, Christian Rieger, and Joseph D. Ward, *An inverse theorem for compact Lipschitz domains for using kernel bases*, Math. Comp. (2016), In press.
- [15] N. Heuer and T. Tran, *Radial basis functions for the solution of hypersingular operators on open surfaces*, Comput. Math. Appl. **63** (2012), no. 11, 1504–1518, DOI 10.1016/j.camwa.2012.03.038. MR2922049
- [16] R. B. Lehoucq and S. T. Rowe, *A radial basis function Galerkin method for inhomogeneous nonlocal diffusion*, Comput. Methods Appl. Mech. Engrg. **299** (2016), 366–380, DOI 10.1016/j.cma.2015.10.021. MR3434919
- [17] F. J. Narcowich, S. T. Rowe, and J. D. Ward, *A novel Galerkin method for solving PDEs on the sphere using highly localized kernel bases*, Math. Comp. **86** (2017), no. 303, 197–231, DOI 10.1090/mcom/3097. MR3557798
- [18] F. J. Narcowich, J. D. Ward, and H. Wendland, *Sobolev bounds on functions with scattered zeros, with applications to radial basis function surface fitting*, Math. Comp. **74** (2005), no. 250, 743–763, DOI 10.1090/S0025-5718-04-01708-9. MR2114646
- [19] F. J. Narcowich, J. D. Ward, and H. Wendland, *Sobolev error estimates and a Bernstein inequality for scattered data interpolation via radial basis functions*, Constr. Approx. **24** (2006), no. 2, 175–186, DOI 10.1007/s00365-005-0624-7. MR2239119
- [20] E. Di Nezza, G. Palatucci, and E. Valdinoci, *Hitchhiker’s guide to the fractional Sobolev spaces*, Bull. Sci. Math. **136** (2012), no. 5, 521–573, DOI 10.1016/j.bulsci.2011.12.004. MR2944369
- [21] R. Schaback, *A unified theory of radial basis functions. Native Hilbert spaces for radial basis functions. II*, J. Comput. Appl. Math. **121** (2000), no. 1-2, 165–177, DOI 10.1016/S0377-0427(00)00345-9. Numerical analysis in the 20th century, Vol. I, Approximation theory. MR1752527
- [22] S. A. Silling, *Linearized theory of peridynamic states*, J. Elasticity **99** (2010), no. 1, 85–111, DOI 10.1007/s10659-009-9234-0. MR2592410
- [23] X. Tian and Q. Du, *Analysis and comparison of different approximations to nonlocal diffusion and linear peridynamic equations*, SIAM J. Numer. Anal. **51** (2013), no. 6, 3458–3482, DOI 10.1137/13091631X. MR3143839
- [24] H. Wendland, *Scattered Data Approximation*, Cambridge Monographs on Applied and Computational Mathematics, vol. 17, Cambridge University Press, Cambridge, 2005. MR2131724

COMPUTATIONAL MATHEMATICS, SANDIA NATIONAL LABORATORIES, ALBUQUERQUE, NEW MEXICO 87185-1320

Email address: rblehou@sandia.gov

DEPARTMENT OF MATHEMATICS, TEXAS A&M UNIVERSITY, COLLEGE STATION, TEXAS 77843

Email address: fnarc@math.tamu.edu

SANDIA NATIONAL LABORATORIES, ALBUQUERQUE, NEW MEXICO 87185

Email address: srowe@sandia.gov

DEPARTMENT OF MATHEMATICS, TEXAS A&M UNIVERSITY, COLLEGE STATION, TEXAS 77843

Email address: jward@math.tamu.edu